International Journal of Legal Medicine (2019) 133:1839–1850
https://doi.org/10.1007/s00414-019-02120-2

METHOD PAPER

Evaluation of the backspatter generation and wound profiles of an anatomically correct skull model for molecular ballistics

Jan Euteneuer[1] · Annica Gosch[1] · Philipp Cachée[2] · Cornelius Courts[1]

Received: 15 February 2019 / Accepted: 2 July 2019 / Published online: 23 July 2019

Abstract

Molecular ballistics connects the molecular genetic analysis of biological traces with the wounding events and complex forensic traces investigated in terminal ballistics. Backspatter, which originates from a projectile hitting a biological target when blood and/or tissue is propelled back into the direction of the gun, is of particular interest; those traces can consolidate and persist on the outer and inner surfaces of firearms and serve as evidence in criminal investigations. Herein, we are the first to present an anatomically correct head model for molecular ballistic research based on a polyurethane skull replica enclosing tissue-simulating sponge material that is doped with "triple-contrast" mixture (EDTA-blood, acrylic paint, and an x-ray contrast agent). Ten percent ballistic gelatin was used as brain simulant. We conducted contact and intermediate-range shots with a Glock 19 pistol (9 mm Luger), a pump-action shotgun (12/70 slugs), and blank cartridge handguns. Each shot was documented by a high-speed camera at 35,000 fps. Apart from the blank cartridge guns, all gunshots penetrated the skull model and created backspatter, which was recovered from the distal part of the barrels and analyzed. The pistol contact shots and one of three shotgun shots yielded full STR profiles. While the shotgun slugs destroyed the skulls, the remaining models could be used for radiological and optical fracture and wound channel evaluation. Known backspatter mechanisms and their respective timing could be confirmed visually by video analysis. Our complete model setup proved to be well applicable to molecular ballistic research as well as wound channel and fracture pattern investigation.

Keywords Molecular ballistics · Backspatter · Ballistic head model · Blank gun

Introduction

Collecting and analyzing biological material from crime scenes are common tasks in forensic case work. In scenarios involving gunshots, blood and tissue from the victim can be propelled out of the entrance wound of the bullet back into the direction of the shooter. This phenomenon later called "backspatter" [1] was already described in the 1930s as of criminological interest when backspatter was found on the shooter's hand [2] as well as on outer and inner surfaces of the gun [3]. The blood pattern distribution from backspatter in general holds clues for the reconstruction of the events and circumstances at the crime scene and thus has been investigated on many occasions including case reenactments [4], experiments with different ballistic models, e.g., bagged blood soaked sponges [5], living cattle [6–8], porcine [9], and even human cadavers [10]. For a long time, though, the systematic molecular analysis of backspatter was rather neglected. Only in recent years, it was demonstrated that backspatter traces from the inside parts the firearm are a viable source of DNA in amounts and quality lending to forensic molecular biological analysis [11, 12]; hence, the term "molecular ballistics" was coined. Subsequently, molecular ballistic backspatter analysis demonstrated its potential for DNA-based victim identification in a real case of triple homicide by gunshot [13]. Furthermore, the simultaneous extraction and analysis of DNA, RNA, and mtDNA from backspatter as well as backspatter analysis for hit zone implication via RNA-mediated trace contextualization have been reported [14, 15].

Electronic supplementary material The online version of this article (https://doi.org/10.1007/s00414-019-02120-2) contains supplementary material, which is available to authorized users.

✉ Cornelius Courts
cornelius.courts@uksh.de

[1] Institute of Forensic Medicine, University Medical Center Schleswig-Holstein, Kiel, Germany

[2] Sachverständigenbüro Cachée, Pistoriusstrasse 6a, 13086 Berlin, Germany

For those experiments and to facilitate comprehensive evaluation of "used" ballistic models and differentiate backspatter within the gun and the wound channel, the "triple-contrast" method involving ballistic models doped with a mix of blood, acrylic paint, and an x-ray contrast agent was devised and validated for molecular ballistic testing [16]. However, up to the present date, the ballistic head models for experimental shootings were made of acrylic spheres [11], plastic boxes [17], polyethylene bottles [14, 16, 18], or casts of ballistic gelatin [19], all doped with bags containing blood or triple-contrast mix and some covered with silicon layers for skin simulants. And while some anatomically correct head models have been studied for fracture development in military research [20–24], so far, no models mimicking the human head in its complex anatomy have been used in backspatter analysis. The development and establishment of an anatomically correct head model for ballistic research are challenging, as it does not only consists the human head of highly heterogeneous and complex structures but it also exhibits a great diversity in the appearances of the scalp [25], skull [26], and brain [27]. To provide for reproducibility of results, standardized synthetic materials are needed reflecting the respective properties of bone and tissue matter that are decisive for the aspect under investigation. Compromises are inevitable, but as long as the results are closely approximate (what can be observed) in reality, simulants do not need to possess the exact same biomechanical attributes and properties as their real counterparts [28].

Herein, we present the first anatomically correct and skull model with realistic features for molecular ballistic testing. To improve reproducibility, we only employed industrially produced items. We aimed to evaluate the model system by subjecting it to a set of different conditions in several different shooting scenarios and address the question whether this model produces realistic backspatter which can then be collected from inner surfaces of different kinds of weapons and be analyzed molecularly biologically, and whether the model produces comparable fracture and wound patterns (proof of concept).

Materials and methods

Blood collection and sample mixture

Blood for the generation of the sample mixture was drawn by venipuncture into sterile EDTA-containing blood collection tubes (Sarstedt, Germany) and was donated solely and voluntarily by one of the authors. The author did not have any contact with the used weapons or ammunition before or during the experimental shooting, nor did he participate in the sample collection or processing. As sample mixture, a "triple-contrast" mixture [16] was freshly prepared with the donated EDTA-blood, acrylic paint (Schmincke, Germany), and Micropaque® contrast agent (Guerbet, Germany) in a ratio of 1:2:2 before assembling the ballistic model.

Preparation of the ballistic model

About 20 mL of the triple-contrast mix was spotted onto a 5 cm × 5 cm × 0.5 cm "dirt eraser" sponge, wrapped in a transparent plastic foil, and sealed in an evacuated vacuum bag (Supp. Fig. 1). This approach of a tissue simulant was preferred over plastic bags with pure liquid, which were used in earlier studies [14, 15, 18] and which were employed here only for comparison (about 5 mL in 4 cm × 4 cm bags). The ability of the soaked "dirt eraser" sponges to produce backspatter in general was confirmed prior to the experimental shooting with a blank cartridge revolver (data not shown).

Commercially available and anatomically correct SYNBONE® skull models with a rubber coating (model number 8880.G, SYNOBONE AG, Switzerland) were washed from the inside with water and 70% ethanol. The gaps at the nasal bone were sealed with hot glue and the foramen ovale and spinosum were tightened with duct tape. Double-sided adhesive tape was used to fix the triple-contrast-filled bags in a target location, i.e., either behind the right temporal bone or the occipital bone, which were chosen for being the most typical target locations for suicidal and homicidal gunshot injuries [29]. The location of the triple-contrast bag was marked with a pen on the corresponding outside spot and the skull models were numbered. Type III ballistic gelatin (Honeywell Fluka™, Germany) was prepared at a 10% concentration following Fackler's instruction [30] and poured into the now liquid-tight skull models through the foramen magnum. The skulls were subsequently stored for 36 h at 4 °C before shooting.

The triple-contrast bag in skull model no. 1 was not fixed directly to the inner surface of the model, but had drifted about 3 cm inside and was completely surrounded by gelatin; the bag of skull 3 had also slightly drifted inwards with its lower half surrounded by gelatin for a few millimeters. This probably happened while pouring the warm liquid gelatin into the skull models and went unnoticed until the shootings were conducted.

Experimental shooting setup and firearms

The experimental shooting was conducted in designated shooting area on the premises of the State Office of Criminal Investigation of Schleswig-Holstein (LKA-SH) in Kiel. The prepared skull models (described above) were fixed at the zygomatic process of the temporal bone with cork lined lab clamps attached to a metal rod on a wooden board, which was always oriented in such a way that the trajectory was leading towards the bullet trap (Supp. Fig. 2). All shots were executed

by a trained professional without stabilization of the weapon to provide for realistic shooting conditions. To avoid contamination and for protection, the shooter was wearing a sterile surgical gown (Lohmann & Rauscher, Germany), standard earloop facemasks (3M Health Care, Germany), a plexiglass helmet, and Micro-Touch® nitrile examination gloves (Ansell, Belgium), which were examined for backspatter traces and changed after each shot.

To represent a variety of relevant firearms, two small arms, a handgun (pistol), and a long gun (single barrel pump action shotgun), as well as blank cartridge handguns freely commercially available in Germany, were employed (Table 1). Bullet entrance location, shooting distance, and the firearm used for each shot are listed in Table 2. Shots to the temporal bone were conducted analogously to typical suicidal shots with the trajectory orientating from the temporal bone diagonally towards the posterior part of the opposite parietal bone. The shots in the occipital bone were orientated in straight direction towards the frontal bone, parallel to the artificial suture left from the manufacturing process. Temperature and humidity were measured shortly before every shot, ranging from 24.7 to 25.5 °C and between 53% and 95% humidity, due to the use of a ventilation system. After each shot, skull models that had not been completely destroyed were carefully transferred into plastic bags and stored at 4 °C.

Video analysis

Video documentation of every shot and the resulting backspatter was done with a Photron FASTCAM SA-Z 2100K high-speed cam at 35,000 fps. Using the Photron FASTCAM Viewer v.3681, a frame-by-frame analysis of every shot was conducted, with every frame representing a time span of 0.029 ms. The time elapsed after bullet entry was taken for the start of the fracture propagation of the skull model, the exit of the bullet, and the different forms of backspatter. In addition, mean bullet velocity was estimated by measuring the wound track (using the CT images) and relating it to the time of passage through the skull model.

Table 2 Target location of each ballistic model

Skull model no.	Matrix	Weapon	Target location	Distance
1	Sponge	P	T	C
2	Sponge	S	T	C
3	Sponge	P	T	5 cm
4	Sponge	S	T	15 cm
5	Liquid	P	T	C
6	Liquid	BR, BP	T	C
7	Sponge	P	O	C
8	Sponge	S	O	C

P, pistol; *S*, shotgun; *BR*, blank revolver; *BP*, blank pistol; *T*, temporal bone; *O*, occipital bone; *C*, contact

Weapon sampling and cleaning procedure

After each firing, the inside of the barrel was sampled using DNA-free forensic nylon swabs (4N6 FLOQ Swabs Crime Scene, Copan Flock Technologies, Italy). Sampling was performed on the distal part of the barrel (approx. 12 cm) at the shotgun and entire barrel at the pistol, using a modified double swab technique [31] employing a single swab with one-half moistened with HPLC gradient grade water (Th. Geyer GmbH & Co. KG, Germany) and one-half dry.

Before using the firearms again, barrels were cleaned with 10% bleach (DanKlorix, Colgate-Palmolive, Germany) and 70% ethanol (Th. Geyer GmbH & Co. KG, Germany) using cotton swabs (Forensic Swabs XL, Sarstedt, Germany) and/or cotton pads (Vereinigte Filzfabriken AG, Germany). After each cleaning, negative controls were taken from the inside of the barrel as described above.

DNA extraction, quantification, and STR profiling

DNA was extracted from the collected samples using the magnetic-bead-based Life Technologies PrepFiler® Forensic DNA Extraction Kit (Thermo Fisher Scientific, USA) according to the manufacturer's instructions resulting in a final elution volume of 50 μL. The DNA concentration and the presence of inhibitors were determined by quantitative PCR

Table 1 Weapon types, firearms, and ammunition

Type	Firearm	Manufacturer	Ammunition	Manufacturer
P	Glock 19	Glock (Austria)	9 mm Full Metal Jacket	GECO (Germany)
S	Pump Gun	Falconetti (Italy)	Practical Slug 12/70 28 g	SAGA (Spain)
BR	Zoraki R1 2.5"	Zoraki (Turkey)	9 mm R.K.	Walther (Germany)
BP	Walther P99 Commando P.A.K.	Walther (Germany)	9 mm P.A. Knall	RUAG (Germany)

P, pistol; *S*, shotgun; *BR*, blank revolver; *BP*, blank pistol

(qPCR) using the PowerQuant® system (Promega, Wisconsin) on an Applied Biosystems™ 7500 fast Realtime PCR System (Thermo Fisher Scientific, USA). Quantification was performed in duplicates following the manufacturer's instructions with 2 μL DNA-containing solution in a reduced reaction volume of 10 μL. This modification to the manufacturer's protocol had been thoroughly validated for routine analysis in our laboratory.

For all samples exhibiting an autosomal DNA quantification value above our internally validated threshold of 0.4 pg/μL, we performed STR multiplex-PCR using the PowerPlex® ESX 17 Fast Kit (Promega, Wisconsin) according to the manufacturer's protocol on an Applied Biosystems™ GeneAmp PCR System 9700 (Thermo Fisher Scientific, USA). PCR products were detected by capillary electrophoresis on an Applied Biosystems™ 3500 Genetic Analyzer (Thermo Fisher Scientific, USA). The resulting data was analyzed with the GeneMapper ID-X software version 1.5 (Thermo Fisher Scientific).

Radiological imaging

Twenty-four hours after shooting, the models were examined by multislice CT (Ingenuity Core, Philips, Netherlands). The scanning was performed with a tube voltage of 120 kV and a tube current of 320 mA in a spiral mode. Reconstructed slice thickness was 0.8 mm with overlapping slices. Reconstruction with a bone and smooth kernel and iterative model reconstruction were performed. The bone kernel was found to be the best reconstruction kernel for the delineation of the concentrated contrast medium versus air versus gelatin in the projectile course. The image post-processing (multiplanar reconstruction with AVG 5-mm slice thickness) was performed on an AGFA Impax workstation EE R20 XVII SU3 v20180419_1405 (AGFA, Belgium) and additionally with InVesalius v3.1.1 (CTI, Brazil).

Skull model and wound channel evaluation

Undestroyed skull models were photographed and documented in terms of skull integrity, fracture patterns, size and shape of entry, and exit wounds as well as soot and triple-contrast deposits. Afterwards, the gelatin brain simulant was extracted from the skull model and cut into ~ 1-cm thick slices perpendicularly to the wound cavity. A scanner (MP C306, Ricoh, Canada) was used to make images of the slices with a resolution of 400 dpi. The images were evaluated with ImageJ 1.52d (NIH, USA) by applying the polygon method [32, 33], where the end of the tears radiating from the wound channel is connected to create a polygon which reflects the maximum extent of the remains of the temporal wound cavity and thus the interconnected dissipated energy from the projectile. The polygon perimeter was determined for every slice to create an impression for the damage along the wound track. This procedure was also applied for the radiological images along the wound track to assess the viability and comparability of both approaches.

Results

Evaluation of high-speed video recordings

The recording of the gunshots with the high-speed camera at 35,000 fps allowed for careful and comprehensive frame-by-frame evaluation of the behavior of the skull model when hit by the bullet as well as backspatter mechanisms and their temporal progress (Table 3; Supp. Table 1). Backspatter was created by every shot, except the blank cartridge gun shots that did not break the "bone." For the other shots, two distinguishable temporally separate modes of backspatter could be observed: an initial first backspattering of gas, bone fragments, and liquid droplets (from the ruptured triple-contrast mix bag) directly following the bullet impact as the entry site bursts open (and thus, we termed "burst" backspatter), and after 6 to 7 ms a second manifestation of backspatter resulting from the collapse of the temporal cavity (which we called analogously "collapse" backspatter). The appearance of both modes is dependent on the actual shooting scenario. Due to accompanying muzzle gases, contact shots with a pistol exhibit a more severe wounding capacity than shots from an intermediate or distant range, and thus cause the first bursting effect, which is absent from distant shot scenarios. The term "contact shot" is employed here, although video images showed that the hard and uneven surface of the skull model whose rubber coat would not efficiently clasp around the muzzle rather provides for an incomplete contact shot scenario.

The destructive force unleashed by the shotgun slugs was sufficient, regardless of shot distance, to instantly destroy the skull model (Fig. 1). Hence, neither "collapse" backspatter nor the exit of the slug could be observed rendering distance estimation impossible. A real close-contact shot also could not be performed as prior to the slugs' exit, the shotgun muzzle was jerked some few millimeters by the recoil, respectively. A gush of triple-contrast mix is thrown into the direction of the shotgun and distributed over the outer surface of the barrel as droplets (skull model no. 2) as well as thick smears of several centimeter length (skull model no. 8). A continuous jet of muzzle gases accompanies the slug and persists for at least 7 ms after bullet entry, pushing small particles and thin droplets away from the muzzle.

The three contact shots fired with the Glock 19 pistol (skull model nos. 1, 5, and 7) generated similar observable patterns of effects in and at the skull models:

Table 3 Measurements from high-speed video recordings

No.	Elapsed time after bullet entry [ms]							
	Fracturing	Bullet exit	"Burst" BS	Appearance	"Collapse" BS	Appearance	l_{WC} [m]	v_B [m/s]
1	0.1	0.5	0.1	Gas, BF	6.5	D	0.160	320
2	0.029	n.m.	0.1	Gas, G, BF	–	–	n.m.	n.m.
3	0.1	0.5	–	–	6.5	D	0.154	308
4	0.029	n.m.	0.1	MSp, G, BF	–	–	n.m.	n.m.
5	0.1	0.5	0.2	Gas, BF, G	6.2	Gas, P	0.158	316
7	0.1	0.6	0.1	Gas, G, MSp, BF	7.0	MSp, D	0.170	283
8	0.029	n.m.	0.1	MSp, G, BF	–	–	n.m.	n.m.

No., skull model number; *BS*, backspatter; *n.m.*, not measurable; *BF*, bone fragments; *D*, droplets; *G*, gush; *MSp*, microspatter spray; *P*, particles (undeterminable); l_{WC}, length of wound channel; v_B, bullet velocity

1. Radial fracturing, originating from the entry site, about 0.1 ms after bullet impact
2. Simultaneous bursting of entry site, with a "burst" backspatter of gas, small bone fragments, and triple-contrast mix from the ruptured bag (Fig. 2)
3. Exit of bullet after 0.5 to 0.6 ms. A tumbled bullet is found at skull 7, with an angle of yaw of about 9.4° (Fig. 2).
4. Bone parts created by radial and secondary concentric fractures arch out and are later either pulled back by elastic force or hurled into the periphery if enough energy had been transferred to rip the rubber coat.
5. Second manifestation of backspatter of droplets, gas, bone particles, or a microspatter spray (Fig. 3) after about 6.2 to 7 ms, following the collapse of the temporal cavity and the (first) pulsating movements of the gelatin.

The backspatter process is thus happening faster than the recoil act (about 55 ms); therefore, the triple-contrast mix was scattered not only on the slide, frame, trigger guard, and the shooter's hand but also on the outside part of the barrel and the recoil spring. The amount of backspatter ending up inside the muzzle could not be estimated due to the lateral view of the camera.

At maximum extent of the entrance holes and before the rubber coat elastically retracts those bone pieces which are still attached to it back into place, the full extent of the oscillation of the ballistic gelatin becomes visible, creating a temporary empty space inside the skulls (Fig. 4). The oscillation continues over the entire length of each video (between 57 ms and 110 ms) and causes the entire skull model to pulsate as well.

As a further observation, skull model no. 5 that was doped with liquid triple-contrast mix in a foil bag exhibited a slightly different generation of backspatter and blood pattern distribution. As a result, after the bullet's impact, the bag was quasi simultaneously flung upwards, ripped apart, and turning round its own axis, thereby releasing the majority of the liquid

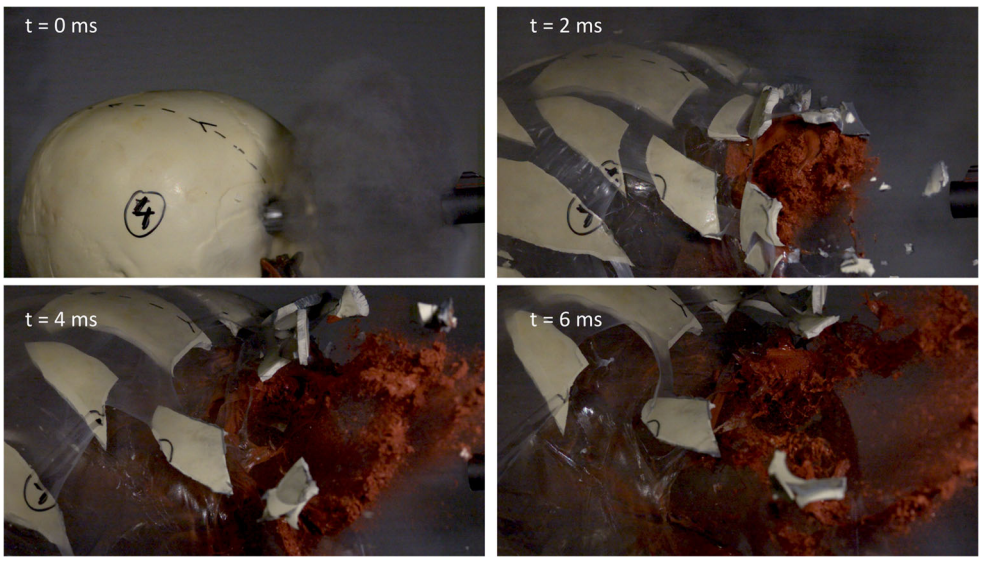

Fig. 1 Destruction of the skull model by the shotgun slug. Explosive character suppresses normal backspatter mechanics

Fig. 2 Shot with 9-mm bullet to the occipital bone, 0.657 ms after impact. Immediate start of "burst" backspatter with colored triple-contrast mix in backstreaming gas. The exiting bullet tumbles with an angle of yaw of about 9.4°

mixture from a few centimeters upside of gun, leaving a thick smear on the upper part of the barrel, the front site of the slide (causing some of the mix being pushed away at the recoil process), and the frame, as well as the upper side of the shooter's thumb and knuckle of his middle finger. With increasing flying distance, the mix is spread out to a net-like structure and finally thins to small drops (in a time span of about 40 ms), resembling the image of a popping water balloon (Fig. 4).

Skull model no. 3 is considered separately as an intermediate shot scenario. After entry of the bullet, the accompanying muzzle gases continue to stream out of the muzzle for about 2 ms and partly enter the wound channel, but mostly are dispersed and deflected from the skull. Without the muzzle gases being injected into the skull as in contact shot setups (thereby significantly contributing to the severity of the damage), the lesser total energy dissipation also results in fewer fracturing and radial cracks of the skull model at and from the entry site. Congruent with the contact shots, it takes about 6.5 ms until the supposed "collapse" backspatter appears. Yet, the intact skull does not allow for an observation of the wound cavity in the gelatin to confirm this. The simultaneous upward jerk of the shooting hand due to the recoil causes the visible backspatter to miss the weapon here (Supp. Fig. 3).

Skull integrity and analyzability

As mentioned above, the models were destroyed by the shotgun slugs rendering the evaluation of the "bony" remains impossible. Still, for some shots, the gelatin brain replicas remained largely intact, thus roughly resembling a Kronlein shot [34] (Supp. Fig. 4). In contrast, shots delivered by pistols left the models fractured but mostly intact. The polyurethane material of the skulls allowed for 3D reconstruction of the scans similar to real bone, but with small adjustments due to its different density.

All three models to which contact shots were delivered exhibited severe bone defects at the entrance wound. Radial and concentric secondary fractures merged and created larger bone pieces which were divulsed away once enough energy had been transferred to rip the rubber coat. The extent of this bone defect was up to a diameter of 10 cm (Supp. Fig. 5 A). Bone defects at the exit sites were smaller, with a maximal diameter of 3.3 cm, yet also exhibited radial and concentric

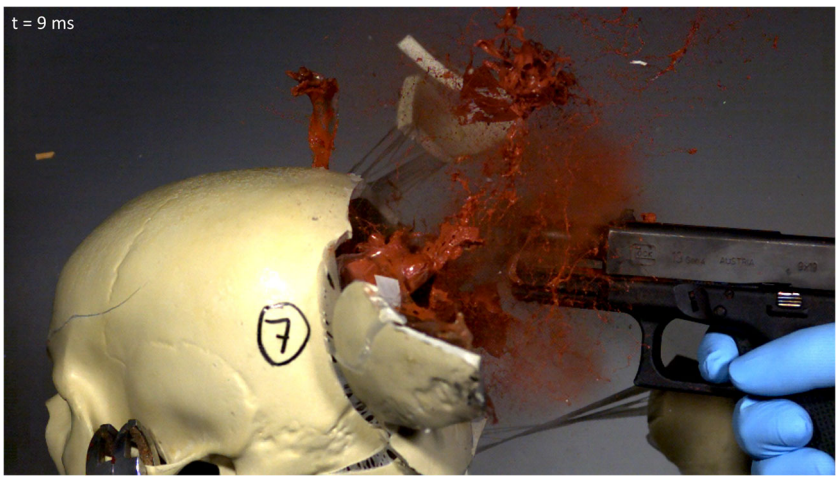

Fig. 3 Shot with 9-mm bullet to the occipital bone, 9 ms after impact. After the "burst" backspatter with gushes of liquid and bone fragments, the "collapse" backspatter streams in direction of the gun as a thick microspatter spray. The inner parts of the gun are exposed to the backspatter due to the recoil process

Fig. 4 Shot with 9-mm bullet to the temporal bone, 20 ms after impact. The liquid-filled bag ripped and gushed upwards, with the triple-contrast mix distributing in an explosive fashion from above. Radial fractures, extensive bone loss at the entry site, and broken zygomatic process of the temporal bone visible. The pulsating brain creates an empty space inside the skull

secondary fractures (Supp. Fig. 5 B). Cratering or external beveling of the bone simulant was only roughly recognizable at the mostly too fragmented entry and exit sites. The zygomatic processes of the temporal bone, where the clamps had been attached, were broken at all three contact shots. When shots to the temporal bone were performed, the fracture propagations were halted at the artificial suture between the hemispheres, which was also torn open by the pressure transmission. Soot deposits were observed in proximity to the bullet entry site and at the malar surface of the zygomatic bone. Stains of the triple-contrast mix in various shapes and sizes were present, but as seen in the high-speed video recordings, originated in part from splashes by the bone fragments which cambered and were then elastically retracted into place by the rubber coat. After fracture documentation, the skulls were opened, and the gelatin brain replicas were removed for wound channel analysis, except for skull model no. 6, which had been shot against the temporal bone with both a blank revolver and a blank pistol. Both shots left distinct soot deposits and small parts of burnt and molten rubber, but did not penetrate the skull (Supp. Fig. 6).

Examination of the wound cavity

The translucent gelatin allowed for a first visual assessment of the bullet track and the distribution of the colored triple-contrast mix. The contact shots at sponge-doped models produced clearly visible colored cracks throughout the wound channel. The shots at models with liquid-only bags produced an uneven distribution of the mixture declining throughout the length of the channel with empty cracks and only very little amounts left in the last half. The distant shot carried even less of the mixture along its path, just filling the cracks for the first ≈ 3 cm and with no visible traces left after 10 cm. Nevertheless, even uncolored cracks and tears were well detectable in the slices cut from the gelatin cores and could be included in the polygon for wound channel analysis. Regardless of the amount of triple-contrast mixture in the model, CT analysis of the wound track was less efficient; a fine resolution adjustment of contrast agent vs. gelatin vs. air could not be achieved; hence, tears and cracks appeared shorter as compared with the optical measurements (Fig. 5). A 3D reconstruction was still possible, however, but also demonstrates less-efficient distribution of the triple-contrast mixture (Supp. Fig. 7). The trends of the polygon perimeter graphs were still quite comparable with the optical evaluation, but produced lower values (Fig. 6). As expected, the graphs show that the damage was greatest after a few centimeters for the models that had received contact shots, due to the added effect of muzzle gas. Without it, at the intermediate shot at skull model no. 3, the damage pattern was similar throughout the entire wound channel. Skull model no. 1 with its inward shifted bag exhibited comparable large temporal cavity before the bag, then a less intense, again first increasing and then decreasing wound profile after the bag.

DNA quantification and STR profiling

DNA quantification and profiling results are listed in Table 4. Negative controls were included to assess the efficiency of the cleaning and sampling procedures. If sufficient material was present that STR profiling could be performed, it always resulted in a full profile from the donor. All pistol contact shots produced full profiles, while samples from intermediate shots failed which was to be expected from the high-speed video recordings showing that the backspatter missed the muzzle. DNA yields varied widely but corresponded to the mechanisms observed in the video recordings as described above: The inward shifted bag from skull model no. 1 produced a lower amount of triple-contrast mixture in the backspatter, and the bag without a sponge (in skull model no. 5) contained a lesser total amount of triple-contrast mix and behaved differently from the bag with a sponge.

Two contamination events were detected. One extra allele was observed in a sample from skull model 1, which may have

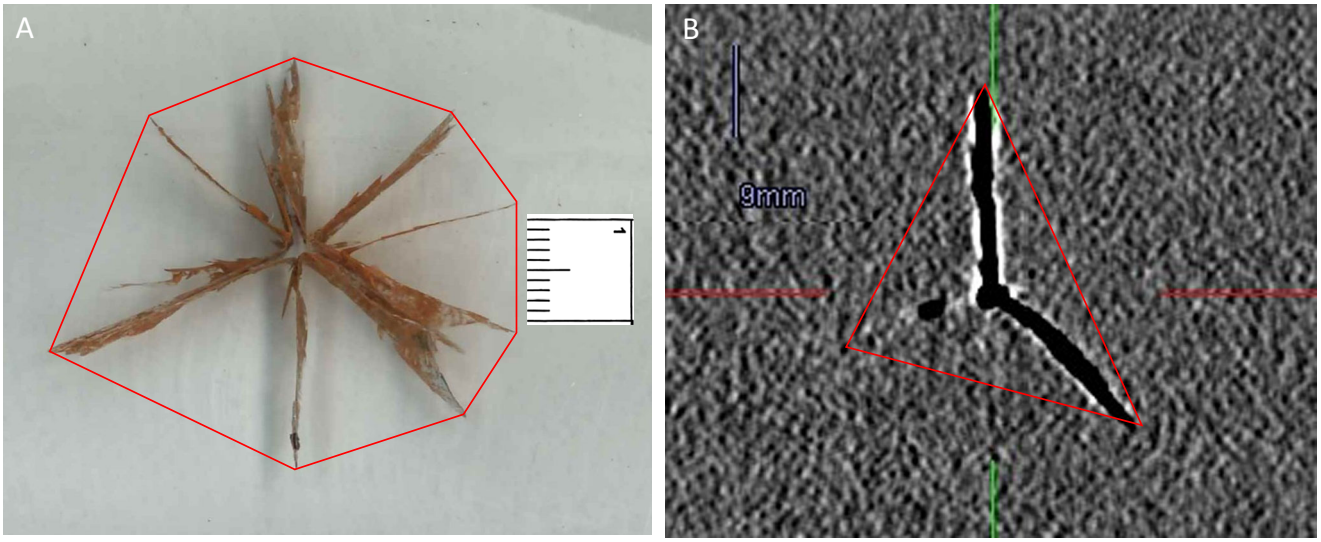

Fig. 5 Examples from wound channel evaluation, the same position is shown with polygon perimeter drawn in red. **a** Scan from 1 cm slice of cut gelatin brain. **b** CT image with 0.537 cm slice thickness, AVG mode

originated from the shooter or the technician, and seven extra alleles appeared in a sample from skull model no. 8, including one allele which could not be related to the profile of any person that had been at the shooting site but may have been present in the gun before the shooting event. Two negative controls also resulted in a full profile, indicating insufficient cleaning after the shot.

Discussion

The applicability and suitability of our new anatomically correct skull model for molecular ballistic research were assessed by testing for the occurrence of backspatter after contact and intermediate shots using two different small arms, evaluating the model's behavior and investigating whether backspatter

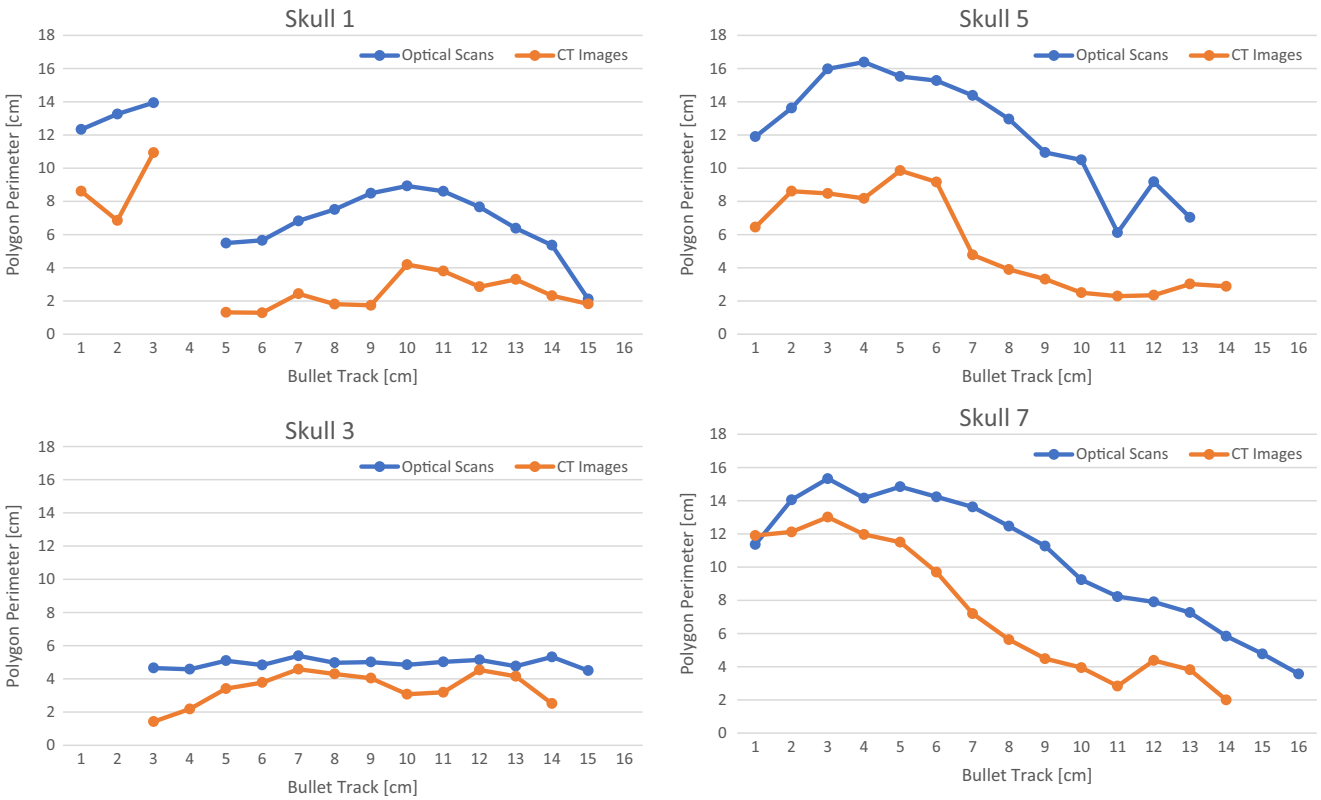

Fig. 6 Comparison of the polygon perimeter method of the four skull models shot with the 9 mm Glock 19

Table 4 Sample quantification and profiling

No.	Type	DNA yield [ng/μL]	STR typing	Full profile donor	Extra alleles
1	P/C	0.0039	+*	Yes	1
1 - neg	P/C	–	n.d.	–	–
2	S/C	–	n.d.	–	–
2 - neg	S/C	–	n.d.	–	–
3	P/C	–	n.d.	–	–
3 - neg	P/C	n.r.	n.d.	–	–
4	S/D	–	n.d.	–	–
4 - neg	S/D	–	n.d.	–	–
5	P/C	0.1192	+	Yes	0
5 - neg	P/C	–	n.d.	–	–
7	P/C	0.2561	+	Yes	0
7 - neg	P/C	0.0034	+	Yes	0
8	S/C	0.0035	+*	Yes	7
8 - neg	S/C	0.0030	+	Yes	0

No., skull model number; *neg.*, negative control after cleaning; *P*, pistol; *S*, shotgun; *C*, contact; *D*, distant; yield, –, < 0.0005; *n.r.*, no result; STR typing, +, 17/17 STR-systems; *n.d.*, not done

*Mixed profile

traces can be collected and analyzed from the inside surfaces of the barrels. To the best of our knowledge, ours is the first model system for molecular ballistic backspatter research which comprises an anatomically correct skull replica with an internal source of biological material embedded into a tissue simulant. We are aware that our model cannot fully simulate a real and highly complex cranial vascular system with dynamic perfusion, which may well be impossible to recreate artificially. Nevertheless, it is an improvement and more realistic than previous model systems albeit accompanied by a more difficult handling and preparation process. Thali et al. when discussing their "skin-skull-brain" model already claimed that an anatomically correct skull model is less reproducible and inter-comparable than spheres [35]. While this may be granted, we argue that striving towards a completer and more realistic model outweighs easier handling. The only failure of model preparation that we encountered was the inward shifted triple-contrast bag (skull model no. 1), which can be obviated by using stronger tape or glue. In fact, the decreased DNA yield in samples from skull model no. 1 highlights the necessity for careful preparation.

Importantly, backspatter was indeed generated by every shot except for the blank cartridge guns. Backspatter traces recovered from the inside surface of the barrel, respectively, after all contact shots with a pistol and from one of three shotgun shots successfully produced STR profiles. Judging from the high-speed videos, the liquid-only bag exhibited a less realistic behavior than the sponge bags. It is safe to assume that this observation does not reflect realistic backspatter behavior, as a comparable cavity of liquid blood is not present inside a human skull. Concerning the nature of the material spattered back from shotgun blows, the "explosive" [36] character of the impact raises the question whether it should be termed "backspatter" at all. Also, taking into account the amount of triple-contrast mix produced by the shotgun blasts and found outside of the barrel, it was not be expected that only one of those samples contained sufficient DNA for STR profiling. Still, FLOQ Swabs have demonstrated low efficiency in sampling "firearm metal" before [37]. The extensive muzzle gases, which dispersed and scattered droplets of backspatter, in combination with a challenging sampling procedure (the greater diameter of the barrel impeded applying sufficient pressure with the swab tips to efficiently recover sample material) probably also contributed to the reduced DNA yield. Additional careful examination of the barrel inside by endoscopy may thus be advisable [17] as well as the application of a more thorough swabbing technique with a barrel-fitting device (e.g., GunSwab C1, Coloprint, Germany). It has to be mentioned that in real cases, all internal parts and surfaces of a gun can and should be sampled [13], whereas herein, we focused on the inside surface of the barrel for uniform comparison. As mentioned above, the backspatter generated by the intermediate shot with the pistol missed the barrel because of the upward jerk of the gun due to recoil. This should be considered for the setup of and regarding the aspect in question in future experiments, e.g., by stabilization of the gun to ensure comparability and if a maximally realistic reenactment including a human shooter affected by recoil of a gunshot scenario is not required.

The measured time span of about 6 ms after which "collapse" backspatter emerged is comparable to the duration of temporary cavity movement in human tissue [38] and also fits to the observations made from 9 mm shots at Sylgard gel, where the first minimal cavity was measured at 6.5 ms after

impact [39]. This resemblance in timing is noteworthy as 10% gelatin exhibits higher elasticity and in general different mechanical properties than brain tissue, which has been argued to restrict its use for specific ballistic research [40]. Falland-Cheung et al. introduced a mix of agar/glycerol/water as a more suitable alternative for brain tissue simulations [41, 42]; however, gelatin still provides the highest comparability with other experiments. The "collapse" backspatter also emerges after contact shots in the form of a microspatter spray about 6–7 ms after impact. This phenomenon can be explained by the muzzle gases extruded into the wound channel and nebulizing the liquid triple-contrast mix when subsequently ejected back through the entrance wound at the collapse of the temporal cavity, an effect which was shown [5] and explained before [43]. Yet, apparently, the major part of backspatter generation is due to the "burst" effect directly after impact. In real comparable contact shots to the head though, the scalp will be tighter and thicker and may withstand higher amounts of transmitted energy without ripping apart as easily as the rubber coat covering our models. Therefore, neither the extent of this effect nor the shape of the wound will closely approximate real cases. As a more severe manifestation, it could roughly be compared with the backspatter effect caused by a subcutaneous gas pocket [44]. Also, the burst entry wound caused the undesired effect of the contrast bag being exposed to the outside and partly destroyed, with its fragments then possibly creating pseudo-backspatter stains on the skull, weapon, and/or hand, or influencing the overall flow of backspatter. An additional stronger skin simulant could be considered for further uses of the model, depending on the focus of research as this would also allow for genuine "hard" contact shots. Rubber coating as periosteum or skin simulant merely acts as a threshold velocity filter [28] and cannot effectively envelop the muzzle, which may also be a reason for the blank cartridge shots having failed to penetrate the skull. Given numerous cases of fatal shots delivered by blank cartridge guns, especially in attempted suicides [45–47] and regarding successful applications of backspatter analysis [12], further experiments may be envisioned.

Wound channel evaluation was possible in skull models after pistol shots, with the optical evaluation outperforming radiological imaging. The quality of the latter obviously correlates with the amount of triple-contrast mix in the bullet track, but also with professional experience in radiological image procession. Similar experiments showed a good correlation between optical and radiological imaging [48]; thus, this additional analytical option should be optimized and not excluded. For the unusual damage pattern at skull model no. 1, it is possible that the bullet had been slowed down by the bag and then deflected or deformed. This remained undecided, however, as neither the shape of the exiting bullet could be discerned from the high-speed video recording nor could the bullet be identified and retrieved from the bullet trap.

Further fracture analysis is well possible with our skull model, but was not focused upon here. A complete destruction/fracturing of the bones by shotgun slugs with ejection of the gelatin brain is comparable to massive injuries encountered in real cases, where the so-called "Kronlein shots" may occur [34, 49], but where skull fragments generally are better held in place by the skin. The fracture development in our model following pistol shots seems in principle comparable to real cases and experiments with handguns, as described in [50, 51]. The artificial suture between the model's hemispheres has yet to be taken into account. Mahoney et al. used Likert-type scaling for the assessment of their polymeric skull models [22], a method which would be applicable for our model as well. SYNBONE polyurethane bone simulants have been used by several groups for gunshot [52, 53] or other experiments [54] and were macroscopically found to behave satisfactorily comparable to human bone, yet acknowledging distinct differences on a microscopic level [55, 56]. The estimated speed of the fracture development comes close to the speed of the bullets, which matches the observations in shots to real cranial bones [57].

According to our observations from the video recordings and the shooting site, there is no distinct correlation between backspatter droplet size and traveling distance, confirming observations of Karger et al. who performed shots to calf heads [58]. The shape of the visible backspatter marks on the gun and hand of the shooter ranged from dots and smears to elongated shapes and "exclamation marks" which can be attributed to the direction of their origin, depending on the velocity and angle at the time of the impact. This is consistent with earlier studies about characteristics of backspatter patterns at close range shots on calves [6] or blood-filled sponges [59].

Conclusion

An anatomically correct skull model comprising a commercially available and standardized SYNBONE skull replica covered with rubber, an internally attached triple-contrast mix (blood – acrylic paint – contrast agent) reservoir as source of trace material, and a core of 10% ballistic gelatin as brain simulant was tested for its usability and suitability in molecular ballistic backspatter research. The model was intended as a closer approximation to and for better comparability with real gunshot scenarios to the head than offered by previous head models. The results were promising and regarded as proof of principle. Backspatter was produced by both pistol and shotgun shots and could successfully be analyzed by forensic DNA profiling. Limitations are conceded in fracturing

simulation and further work is needed to optimize the difficult preparation process.

Acknowledgments We, again, are very grateful to the Landeskriminalamt Schleswig-Holstein for facilitating and friendly helping the experimental shooting session on their premises. We also thank Jasper Schupp (Department of Radiology and Neuroradiology, UKSH Kiel) for performing the CT imaging and his aid with radiological evaluation. Special thanks go to Thomas Meier of "VKT Video Kommunikation GmbH – Technisches Fernsehen," for providing the high-speed camera and helping to create truly excellent slow-motion captures. The expert technical assistance of Katharina "Sternenstaub" Pöhls is also gratefully acknowledged.

Funding information This project was funded by the Deutsche Forschungsgemeinschaft (DFG) (CO 992/7-1).

References

1. Stephens BG, Allen TB (1983) Back spatter of blood from gunshot wounds—observations and experimental simulation. J Forensic Sci 28(2):11526J. https://doi.org/10.1520/JFS11526J
2. Weimann W (1931) Über das Verspritzen von Grewebsteilen aus Einschußöffnungen und seine kriminalistische Bedeutung. Dtsch Z Ges Gerichtl Med 17(1):92–105. https://doi.org/10.1007/BF02252047
3. Brüning A, Wiethold F (1934) Die Untersuchung und Beurteilung von Selbstmörderschußwaffen. Dtsch Z Ges Gerichtl Med 23(S2): 71–82. https://doi.org/10.1007/BF01771912
4. Yen K, Thali MJ, Kneubuehl BP, Peschel O, Zollinger U, Dirnhofer R (2003) Blood-spatter patterns: hands hold clues for the forensic reconstruction of the sequence of events. Am J Forensic Med Pathol 24(2):132–140. https://doi.org/10.1097/01.paf.0000065164.92878.2f
5. Kunz SN, Brandtner H, Meyer HJ (2015) Characteristics of backspatter on the firearm and shooting hand—an experimental analysis of close-range gunshots. J Forensic Sci 60(1):166–170. https://doi.org/10.1111/1556-4029.12572
6. Karger B, Nüsse R, Bajanowski T (2002) Backspatter on the firearm and hand in experimental close-range gunshots to the head. Am J Forensic Med Pathol 23(3):211–213. https://doi.org/10.1097/01.PAF.0000022883.79132.77
7. Karger B (1995) Penetrating gunshots to the head and lack of immediate incapacitation. I Wound ballistics and mechanism of incapacitation. Int J Leg Med 108(2):53–61. https://doi.org/10.1007/BF01369905
8. Karger B (1995) Penetrating gunshots to the head and lack of immediate incapacitation. II Review of case reports. Int J Leg Med 108(2):53–61. https://doi.org/10.1007/BF01369905
9. Radford GE, Taylor MC, Kieser JA, Waddell JN, Walsh KAJ, Schofield JC, Das R, Chakravorty E (2016) Simulating backspatter of blood from cranial gunshot wounds using pig models. Int J Legal Med 130(4):985–994. https://doi.org/10.1007/s00414-015-1219-x
10. Rossi C, Herold LD, Bevel T, McCauley L, Guadarrama S (2017) Cranial backspatter pattern production utilizing human cadavers. J Forensic Sci 63:1526–1532. https://doi.org/10.1111/1556-4029.13713
11. Courts C, Madea B, Schyma C (2012) Persistence of biological traces in gun barrels–an approach to an experimental model. Int J Legal Med 126(3):391–397. https://doi.org/10.1007/s00414-011-0655-5
12. Schyma C, Madea B, Courts C (2013) Persistence of biological traces in gun barrels after fatal contact shots. Forensic Sci Int Genet 7(1):22–27. https://doi.org/10.1016/j.fsigen.2012.05.008
13. Courts C, Gahr B, Madea B, Schyma C (2014) Persistence of biological traces at inside parts of a firearm from a case of multiple familial homicide. J Forensic Sci 59(4):1129–1132. https://doi.org/10.1111/1556-4029.12434
14. Grabmüller M, Schyma C, Euteneuer J, Madea B, Courts C (2015) Simultaneous analysis of nuclear and mitochondrial DNA, mRNA and miRNA from backspatter from inside parts of firearms generated by shots at "triple contrast" doped ballistic models. Forensic Sci Med Pathol 11(3):365–375. https://doi.org/10.1007/s12024-015-9695-3
15. Lux C, Schyma C, Madea B, Courts C (2014) Identification of gunshots to the head by detection of RNA in backspatter primarily expressed in brain tissue. Forensic Sci Int 237:62–69. https://doi.org/10.1016/j.forsciint.2014.01.016
16. Schyma C, Lux C, Madea B, Courts C (2015) The 'triple contrast' method in experimental wound ballistics and backspatter analysis. Int J Legal Med 129(5):1027–1033. https://doi.org/10.1007/s00414-015-1151-0
17. Schyma C, Bauer K, Brünig J, Courts C, Madea B (2017) Staining in firearm barrels after experimental contact shots. Forensic Sci Int 273:64–70. https://doi.org/10.1016/j.forsciint.2017.01.031
18. Grabmüller M, Cachée P, Madea B, Courts C (2016) How far does it get?–the effect of shooting distance and type of firearm on the simultaneous analysis of DNA and RNA from backspatter recovered from inside and outside surfaces of firearms. Forensic Sci Int 258:11–18. https://doi.org/10.1016/j.forsciint.2015.10.030
19. Schyma C, Bauer K, Brünig J (2017) The reference cube. A new ballistic model to generate staining in firearm barrels. Forensic Sci Med Pathol 13(2):188–195. https://doi.org/10.1007/s12024-017-9868-3
20. Freitas CJ, Mathis JT, Scott N, Bigger RP, MacKiewicz J (2014) Dynamic response due to behind helmet blunt trauma measured with a human head surrogate. Int J Med Sci 11(5):409–425. https://doi.org/10.7150/ijms.8079
21. Carr D, Lindstrom A-C, Jareborg A, Champion S, Waddell N, Miller D, Teagle M, Horsfall I, Kieser J (2015) Development of a skull/brain model for military wound ballistics studies. Int J Legal Med 129(3):505–510. https://doi.org/10.1007/s00414-014-1073-2
22. Mahoney PF, Carr DJ, Delaney RJ, Hunt N, Harrison S, Breeze J, Gibb I (2017) Does preliminary optimisation of an anatomically correct skull-brain model using simple simulants produce clinically realistic ballistic injury fracture patterns? Int J Legal Med 131(4): 1043–1053. https://doi.org/10.1007/s00414-017-1557-y
23. Mahoney P, Carr D, Arm R, Gibb I, Hunt N, Delaney RJ (2018) Ballistic impacts on an anatomically correct synthetic skull with a surrogate skin/soft tissue layer. Int J Legal Med 132(2):519–530. https://doi.org/10.1007/s00414-017-1737-9
24. Mahoney P, Carr D, Harrison K, McGuire R, Hepper A, Flynn D, Delaney RJ, Gibb I (2018) Forensic reconstruction of two military combat related shooting incidents using an anatomically correct synthetic skull with a surrogate skin/soft tissue layer. Int J Legal Med 133:151–162. https://doi.org/10.1007/s00414-018-1802-z
25. Hori H, Moretti G, Rebora A, Crovato F (1972) The thickness of human scalp: Normal and bald. J Investig Dermatol 58(6):396–399. https://doi.org/10.1111/1523-1747.ep12540633
26. de Boer HHH, van der Merwe AEL, Soerdjbalie-Maikoe VV (2016) Human cranial vault thickness in a contemporary sample of 1097 autopsy cases: relation to body weight, stature, age, sex and ancestry. Int J Legal Med 130(5):1371–1377. https://doi.org/10.1007/s00414-016-1324-5
27. Reardon PK, Seidlitz J, Vandekar S, Liu S, Patel R, Park MTM, Alexander-Bloch A, Clasen LS, Blumenthal JD,

Lalonde FM, Giedd JN, Gur RC, Gur RE, Lerch JP, Chakravarty MM, Satterthwaite TD, Shinohara RT, Raznahan A (2018) Normative brain size variation and brain shape diversity in humans. Science 360(6394):1222–1227. https://doi.org/10.1126/science.aar2578

28. Jussila J, Leppäniemi A, Paronen M, Kulomäki E (2005) Ballistic skin simulant. Forensic Sci Int 150(1):63–71. https://doi.org/10.1016/j.forsciint.2004.06.039
29. Karger B, Billeb E, Koops E, Brinkmann B (2002) Autopsy features relevant for discrimination between suicidal and homicidal gunshot injuries. Dtsch Z Ges Gerichtl Med 116(5):273–278. https://doi.org/10.1007/s00414-002-0325-8
30. Fackler ML, Malinowski JA (1988) Ordnance gelatin for ballistic studies. Detrimental effect of excess heat used in gelatin preparation. Am J Forensic Med Pathol 9(3):218–219
31. Pang BCM, Cheung BKK (2007) Double swab technique for collecting touched evidence. Leg Med (Tokyo) 9(4):181–184. https://doi.org/10.1016/j.legalmed.2006.12.003
32. Schyma CWA (2010) Colour contrast in ballistic gelatine. Forensic Sci Int 197(1–3):114–118. https://doi.org/10.1016/j.forsciint.2010.01.002
33. Schyma C, Madea B (2012) Evaluation of the temporary cavity in ordnance gelatine. Forensic Sci Int 214(1–3):82–87. https://doi.org/10.1016/j.forsciint.2011.07.021
34. Krönlein RU (1899) Beitrag zur Lehre der Schädel-Hirnschüsse aus unmittelbarer Nähe mittels des schweizerischen Repetiergewehrs Modell 1889. Arch Klin Chir 59:67–76
35. Thali MJ, Kneubuehl BP, Zollinger U, Dirnhofer R (2002) The "skin–skull–brain model". A new instrument for the study of gunshot effects. Forensic Sci Int 125(2–3):178–189. https://doi.org/10.1016/S0379-0738(01)00637-5
36. Butler EG, Puckett WO, Harvey EN, McMillen JH (1945) Experiments on head wounding by high velocity missiles. J Neurosurg 2(4):358–363. https://doi.org/10.3171/jns.1945.2.4.0358
37. Wood I, Park S, Tooke J, Smith O, Morgan RM, Meakin GE (2017) Efficiencies of recovery and extraction of trace DNA from non-porous surfaces. Forensic Sci Int Genet Suppl Ser 6:e153–e155. https://doi.org/10.1016/j.fsigss.2017.09.022
38. Karger B (2008) Forensic ballistics. In: Tsokos M (ed) Forensic pathology reviews, Volume 5, 1. Aufl., vol 5. Humana Press, s.l., pp 139–172
39. Zhang J, Yoganandan N, Pintar FA, Gennarelli TA (2005) Temporal cavity and pressure distribution in a brain simulant following ballistic penetration. J Neurotrauma 22(11):1335–1347. https://doi.org/10.1089/neu.2005.22.1335
40. Lazarjan MS, Geoghegan PH, Jermy MC, Taylor M (2014) Experimental investigation of the mechanical properties of brain simulants used for cranial gunshot simulation. Forensic Sci Int 239:73–78. https://doi.org/10.1016/j.forsciint.2014.03.022
41. Falland-Cheung L, Waddell JN, Lazarjan MS, Jermy MC, Winter T, Tong D, Brunton PA (2017) Use of agar/glycerol and agar/glycerol/water as a translucent brain simulant for ballistic testing. J Mech Behav Biomed Mater 65:665–671. https://doi.org/10.1016/j.jmbbm.2016.09.034
42. Falland-Cheung L, Scholze M, Hammer N, Waddell JN, Tong DC, Brunton PA (2018) Elastic behavior of brain simulants in comparison to porcine brain at different loading velocities. J Mech Behav Biomed Mater 77:609–615. https://doi.org/10.1016/j.jmbbm.2017.10.026
43. Peschel O, Kunz SN, Rothschild MA, Mützel E (2011) Blood stain pattern analysis. Forensic Sci Med Pathol 7(3):257–270. https://doi.org/10.1007/s12024-010-9198-1
44. Karger B, Nüsse R, Brinkmann B et al (1996) Backspatter from experimental close-range shots to the head. Int J Legal Med 109(2):66–74. https://doi.org/10.1007/BF01355519
45. Giese A, Koops E, Lohmann F, Westphal M, Püschel K (2002) Head injury by gunshots from blank cartridges. Surg Neurol 57(4):268–277. https://doi.org/10.1016/S0090-3019(02)00643-2
46. Buyuk Y, Cagdir S, Avsar A, Duman GU, Melez DO, Sahin F (2009) Fatal cranial shot by blank cartridge gun. Two suicide cases. J Forensic Legal Med 16(6):354–356. https://doi.org/10.1016/j.jflm.2009.01.011
47. Demirci S, Dogan KH, Koc S (2011) Fatal injury by an unmodified blank pistol. A case report and review of the literature. J Forensic Legal Med 18(6):237–241. https://doi.org/10.1016/j.jflm.2011.05.005
48. Schyma C, Greschus S, Urbach H, Madea B (2012) Combined radio-colour contrast in the examination of ballistic head models. Dtsch Z Ges Gerichtl Med 126(4):607–613. https://doi.org/10.1007/s00414-012-0704-8
49. Karger B, Banaschak S (1997) Two cases of exenteration of the brain from Brenneke shotgun slugs. Int J Legal Med 110(6):323–325. https://doi.org/10.1007/s004140050096
50. Madea B, Staak M (1988) Determination of the sequence of gunshot wounds of the skull. J Forensic Sci Soc 28(5–6):321–328. https://doi.org/10.1016/S0015-7368(88)72858-3
51. Viel G, Gehl A, Sperhake JP (2009) Intersecting fractures of the skull and gunshot wounds. Case report and literature review. Forensic Sci Med Pathol 5(1):22–27. https://doi.org/10.1007/s12024-008-9062-8
52. Bir C, Andrecovich C, DeMaio M, Dougherty PJ (2016) Evaluation of bone surrogates for indirect and direct ballistic fractures. Forensic Sci Int 261:1–7. https://doi.org/10.1016/j.forsciint.2016.01.023
53. Bolliger SA, Ampanozi G, Kneubuehl BP, Thali MJ (2014) Gunshot to the pelvis – experimental ballistics and forensic radiology. J Forensic Radiol Imaging 2(1):17–19. https://doi.org/10.1016/j.jofri.2013.12.001
54. Zwirner J, Bayer R, Japes A, Eplinius F, Dreßler J, Ondruschka B (2017) Suicide by the intraoral blast of firecrackers - experimental simulation using a skull simulant model. Int J Legal Med 131(6):1581–1587. https://doi.org/10.1007/s00414-017-1580-z
55. Smith MJ, James S, Pover T, Ball N, Barnetson V, Foster B, Guy C, Rickman J, Walton V (2015) Fantastic plastic? Experimental evaluation of polyurethane bone substitutes as proxies for human bone in trauma simulations. Legal Med 17(5):427–435. https://doi.org/10.1016/j.legalmed.2015.06.007
56. Taylor SC, Kranioti EF (2018) Cranial trauma in handgun executions: experimental data using polyurethane proxies. Forensic Sci Int 282:157–167. https://doi.org/10.1016/j.forsciint.2017.11.032
57. Sellier K (1982) Schusswaffen und Schusswirkungen, 2., neubearb. u. erw. Aufl. Arbeitsmethoden der medizinischen und naturwissenschaftlichen Kriminalistik, Bd. 8. Schmidt-Römhild, Lübeck
58. Karger B, Nüsse R, Tröger HD, Brinkmann B (1997) Backspatter from experimental close-range shots to the head. Int J Legal Med 110(1):27–30. https://doi.org/10.1007/BF02441022
59. Kunz SN, Brandtner H, Meyer H (2013) Unusual blood spatter patterns on the firearm and hand: a backspatter analysis to reconstruct the position and orientation of a firearm. Forensic Sci Int 228(1–3):e54–e57. https://doi.org/10.1016/j.forsciint.2013.02.012